Natural Resources Canada Ressources naturelles Canada

GEOLOGICAL SURVEY OF CANADA
OPEN FILE 7814

Implicit 3-D modelling of geological surfaces with the Generalized Radial Basis Functions (GRBF) algorithm

M.J. Hillier, E.A. de Kemp, and E.M. Schetselaar

2017

GEOLOGICAL SURVEY OF CANADA
OPEN FILE 7814

Implicit 3-D modelling of geological surfaces with the Generalized Radial Basis Functions (GRBF) algorithm

M.J. Hillier, E.A. de Kemp, and E.M. Schetselaar

2017

Permanent link: https://doi.org/10.4095/301665

This publication is available for free download through GEOSCAN (http://geoscan.nrcan.gc.ca/).

Recommended citation
Hillier, M.J., de Kemp, E.A., and Schetselaar, E.M., 2017. Implicit 3-D modelling of geological surfaces with the Generalized Radial Basis Functions (GRBF) algorithm; Geological Survey of Canada, Open File 7814, 15 p. https://doi.org/10.4095/301665

Publications in this series have not been edited; they are released as submitted by the author.

Abstract

We summarize an interpolation algorithm, which was developed to model 3D geological surfaces, and its application to modelling regional stratigraphic horizons in the Purcell basin, a study area in the SEDEX project under the Targeted Geoscience Initiative 4 program. We developed a generalized interpolation framework using Radial Basis Functions (RBF) that implicitly models 3D continuous geological surfaces from scattered multivariate structural data. The general form of the mathematical framework permits additional geologic information to be included in the interpolation in comparison to traditional interpolation methods using RBF's such as: (1) stratigraphic data from above and below targeted horizons (2) modelled anisotropy and (3) orientation constraints (e.g. planar and linear).

Introduction

Models of 3D geological surfaces provide valuable information of the subsurface commonly used in earth resource exploration. Currently, explicit and implicit surface modelling approaches are used to model 3D geological surfaces (Caumon et al., 2007). Important differences between the approaches are: (1) the explicit approach is only concerned with the particular surfaces being modelled whereas the implicit approach models entire volumes; and (2) the explicit approach is more interpretative and driven by user-based modelling decisions and models are not reproducible whereas the implicit approach is more data driven and models are reproducible. The latter approach is used in this paper.

In the past, high computational costs were normally associated with implicit approaches due to the fact that a single mathematical function, a linear sum consisting of as many terms as there are data points, is fitted by solving a system of equations. Furthermore, to visualize the modelled result the function has to be evaluated at every point in a 3D grid. Therefore, as the number of data points increases, the corresponding set of computational resources required to fit and evaluate the function in reasonable times significantly increases. However, as a result of Moore's Law (Moore, 1965), computational resources have expanded exponentially. In addition, significant progress made in numerical methods (e.g. matrix solvers, fast evaluators, domain decomposition methods) permit the use of implicit approaches to be applied on data sets containing up to millions of points (Beatson et al., 2000; Cuomo et al., 2013).

In implicit modelling, the fitted mathematical function describes a scalar field typically representing a signed distance from a surface defined by a scalar function $f(\boldsymbol{x}) = 0$ where $\boldsymbol{x}$ is a 3D position vector. Following the evaluation of the function in a 3D grid, a surface is triangulated by tracing everywhere the scalar field is zero by using a marching cube (Lorensen and Cline, 1987) or marching tetrahedral (Treece et al., 1999) algorithm. The major advantage of implicit modelling is that very complex surfaces can be accurately modelled from scattered data sampling. However, current implicit radial basis function (RBF) approaches (Turk and O'Brien, 1999; Carr et al., 2001), when applied to modelling geological surfaces from sparse data suffer from the following four limitations: (1) Artificial offset points are required to specify local geometry. Using local normal measurements, offset points are projected above and below surface points and their corresponding scalar field are respectively defined as $f(\boldsymbol{x}) = 1$ (above) and $f(\boldsymbol{x}) = -1$ (below). The magnitude by which they are projected is a user-specified parameter. This characteristic can create significant issues in largely varying structures such as isoclinal folding since an offset point may be projected on the incorrect side of a fold causing topological problems. (2) Common lithological constraints, such as markers that are stratigraphically above or below particular geological contacts are not included. (3) Strike/dip observations with polarity are not included. (4) Data mined structural anisotropy are not incorporated. Our developed generalized radial basis function algorithm (GRBF) overcomes all aforementioned limitations.

Results

GRBF algorithm

The GRBF algorithm, written in the C++ programming language, was incorporated into GoCad/SKUA, a sophisticated geological modelling application, as a plugin. GRBF plugins for GoCad/SKUA versions 2011.2p2 and 2013.2 have been developed. The 2013.2 plugin has a user-interface illustrated in Figure 1.

This section of the paper is organized as follows. First, a detailed description of the input data used by the algorithm is given. Second, the sequence of steps performed by the algorithm is described. Third, advanced modelling parameters are explained. Finally, applications of the GRBF algorithm in various geological settings with varying degrees of structural complexity are shown.

Input data

The types of geological observations used by the algorithm are shown in Figure 2. On-contact constraints are sampled 3D point locations of the geological surface and can come from outcrop or drill core information. Gradient constraints encapsulate strike/dip with polarity (younging direction) observations sampling planar orientations of contact surfaces or off-contact horizons. Tangent constraints are linear orientation constraints of lines tangent to stratigraphic horizons (e.g. apparent dip and fold axes constraints). Inequality constraints are sampled 3D point locations above or below a particular geological surface.

Algorithm steps

The algorithm first constructs a system of equations using the inputted set of geological observations and solves the system for weight coefficients, w_j, from the following mathematical function called the interpolant:

$$s(\boldsymbol{x}) = \sum_{j}^{N} w_j \, \lambda_j^{\boldsymbol{x}'} \varphi(\boldsymbol{x}, \boldsymbol{x}') + p(\boldsymbol{x})$$

where $\lambda_j^{\boldsymbol{x}'}$ are linear functionals acting on a radial basis function $\varphi(\boldsymbol{x}, \boldsymbol{x}')$ with respect to $\boldsymbol{x}' = (x', y', z')$ (a 3D position vector) and $p(\boldsymbol{x})$ is a low degree polynomial. Note that all of mathematical and implementation details of the algorithm can be found in Hillier et al. (2014). For the second step, determined weight coefficients are used to evaluate the interpolant everywhere in a 3D grid to compute the scalar field. As an example, the scalar field for a synthetic anticlinal structure with sampled on-contact point locations and off-contact gradient constraints is illustrated in Figure 3. The third and final step of the algorithm uses a marching cube technique to triangulate the surface everywhere the computed scalar field is zero.

Advanced options

The advanced options section of the user interface (Figure 1) contains options that can largely affect the modelled results and improve the computation speed. Each advanced option is described in this section.

Densify gradient constraints

The "densify gradient constraints" option will attempt to remove any topological errors, such as holes, in modelled surfaces. These types of errors can occur in localized dense sampling of on-contact points possessing large structural variability. Figure 4 illustrates topological errors that can be produced in modelled surfaces and the effect of using the "densify gradient constraints" to rectify such errors. When this option is selected the set of strike/dip with polarity observations are used to estimate the normal vector (gradient) at on-surface observations where there are no structural measurements. The estimated normal vector attempts to correctly assign the polarity and its direction of the scalar field at on-surface points to force modelled surfaces to be topologically consistent across the entire model space.

Domain decomposition

The "domain decomposition" option can significantly improve computations times. As an example, for a data set including 149 on-contact, 53 inequality, and 164 gradient points and using a 1.6 million cell 3D grid, the total algorithm computation time was improved by 360 times (5 hours to 50 seconds) when using this option. The partition of unity method (Babuska and Melenk, 1997) was used for the domain decomposition method because it was flexible enough to be used within the mathematical framework developed in this project. The basis of the method involves breaking the problem into many smaller problems. This is accomplished by using a kd-tree data structure (Bentley, 1975) to subdivide the 3D space into smaller rectangular sub-domains as illustrated in Figure 5a. Local data sets are assigned to each sub-domain which overlaps neighbouring sub-domains. These data sets are determined by finding all data points that are contained within a sphere positioned at the center of the subdomain. Sphere radii are chosen such that at a minimum the sphere will enclose the rectangular subdomain, illustrated in Figure 5b. Separate interpolants are then determined for each sub-domain using local data sets. To compute the scalar field at a particular point in space (green star in Figure 5b) all interpolants whose sub-domain's sphere overlaps the evaluation point gets used to smoothly blended multiple interpolant results together.

Global Plunge Modelling

The global plunge modelling option can be used to incorporate data-mined or user-specified global anisotropy. Modelling of geological surfaces with incorporated anisotropy significantly enhances smoothness of surfaces oriented in the direction of anisotropy. In effect, this maintains fold hinges up and down fold axes away from data to model more geologically realistic surfaces. That can be demonstrated in the LMC (Lower Aldridge-Middle Aldridge contact) horizon in to Purcell Basin as shown in Figure 6.

Smoothing

The "smoothing" option changes modelled results from being an interpolation (fits input data exactly) to an approximation. Larger smoothing values introduce larger residuals in order to obtain smoother modelled results. Smoothing is particularly useful when using noisy data or data characterized by large uncertainties.

Matrix Solver

The purpose of the "matrix solver" option is to give the user access to a faster, although less precise, matrix solver known as GMRES (generalized minimal residual method) (Saad and Schultz, 1986) over the default solver which uses the traditional lower upper (LU) decomposition method. When the GMRES method is selected the user will have to provide the total percentage error permitted into the final solution. Since the solver is not required to solve the system of equations exactly, the computational time needed to find a solution with some error is significantly reduced. Coincidently, this option also acts as a smoothing mechanism.

Sample GRBF results

To demonstrate the applicability and flexibility of the GRBF algorithm in various geological settings with varying degrees of structural complexity a number of examples are given. In the first example, illustrated in Figure 7, a complex synthetic fold is modelled using the algorithm. Demonstrated in the results is the improvement of the modelled surface's geometry when inequality constraints are included in the solution. In general, adding lithostratigraphic observations above or below targeted geological contacts in the form of inequality constraints enhances structural variability in modelled results. These enhancements provide more accurate representations of the geology. Another example of these enhancements is shown in Figure 8, a small region from the Purcell basin, also illustrates improvements of modelled geometry where there are many inequality constraints available. In the final example, shown in Figure 9, an intrusion is modelled from point data sampling inside, outside, and boundary locations.

3D Structural Modelling of the Purcell Basin

The GRBF algorithm presented in this paper was used to visualize and predict the upper and Lower Aldridge Formation contact, a key stratigraphic target horizon and host of the Sullivan Zn-Pb-Ag deposit within the Purcell Anticlinorium, Southern British Columbia, Canada. This work was a project under the Targeted Geoscience Initiative (TGI) 4 program. One of the outputs for the project was a regional 3D structural model constructed from map-based structural and stratigraphic information, regional geophysics, and limited borehole data. The dimensions of the model were roughly equal to 98 km wide by 112 km long by 15 km depth. The GRBF algorithm was a key component in constructing the fault network and stratigraphic horizons in the regional structural model.

Individual fault surfaces in the Purcell Basin were modelled separately. Typically, each fault was modelled using interpretative map traces of the fault in addition to very limited structural observation data at surface. In a few instances, locations of faults at depth were derived from seismic profiles clearly indicating the presence of faults. Using SKUA the set of fault surfaces were properly cut using user specified topological relationships. Figure 10a shows the final modelled fault network.

Key stratigraphic horizons were modelled separately within each modelled fault domain using the appropriate structural and stratigraphic data from its domain. Portions of modelled surfaces far away from data were removed, as can be seen in Figure 10b, resulting in an incomplete covering over the model space. These portions were removed because the remaining stratigraphic horizon patches, possessing higher levels of confidence, will act as data constraints in the final stage of the modelling process. The complete set of modelled stratigraphic horizon patches and fault network are then used in a SKUA workflow that employs a UVT transformation (Mallet, 2004) to generate a complete 3D structural model topologically consistent throughout the model space (even across faults). The final model is shown in Figure 11.

Discussion/Models

The GRBF algorithm was a tool developed with the goal to implicitly model 3D structural geologic surfaces on regional scales using sparsely scattered structural observations. Currently there are no tools or software implementing implicit approaches specifically developed for 3D geological modelling on regional scales using sparse data. The future of mineral exploration will increasingly need such tools to reduce risk (both from economical and geotechnical perspectives) and to find deeper ore deposits.

Further research and development is needed to make increasingly more sophisticated tools which incorporate all available geological data and expert knowledge to obtain more quantitative representations of the regional geology. The algorithm presented in this paper is capable of modelling 3D geological surfaces reasonably well in most circumstances, as can be shown from the 3D structural models of the Purcell Basin (Figure 11). There are, however, many more modelling capabilities that are needed to produce more geological realistic and accurate models. Future work involves enhancing the algorithm to model multiple surfaces simultaneously and to incorporate geological rules such as stratigraphic relationships.

Implications for Exploration

The GRBF algorithm provides geoscientists with a set of tools that can enhance their current understanding of the regional geometry of key stratigraphic horizons, especially in regions with sparse or no data. In areas where key stratigraphic horizons host ore deposits, such as the Zn-Pb-Ag deposit within the Purcell Anticlinorium, modelled horizons have the potential to guide drilling campaigns and yield new ore deposit discoveries.

References

Babuska, I., and Melenk, J.M., 1997, The partition of unity method: International Journal for Numerical Methods in Engineering, v. 40, p. 727-758.

Beatson, R.K., Light, W.A., and Billings, S., 2000, Fast solution of the radial basis function interpolation equations: domain decomposition methods: Society for Industrial and Applied Mathematics, Journal on Scientific Computing, v. 22, p. 1717–1740.

Bentley, J.L., 1975, Multidimensional binary search trees used for associative searching: Communications of the Association for Computing Machinery, v. 18(9), p. 509-517.

Carr, J.C., Beatson, R.K., Cherrie, J.B., Mitchell, T.J., Fright, W.R., McCallum, B.C., and Evans, T.R., 2001, Reconstruction and representation of 3D objects with radial basis functions, *in* ACM SIGGRAPH 2001, Computer graphics proceedings: ACM Press, New York, p. 67–76.

Caumon, G., Antoine, C., and Tertois, A.L., 2007, Building 3D geological surfaces from field data using implicit surfaces, *in* Proceedings of the 27th Gocad Meeting, Nancy, France.

Cuomo, S., Galletti, A., Giunta, G., and Starace, A., 2013, Surface reconstruction from scattered point via RBF interpolation on GPU, *in* 2013 Federated Conference on Computer Science and Information Systems, p. 433-440

Hillier, M., Schetselaar, E., de Kemp, E., and Perron, G., 2014, Three-Dimensional Modelling of Geological Surfaces Using Generalized Interpolation with Radial Basis Functions: Mathematical Geology, v. 46, p. 931-953.

Lorensen, W.E., and Cline, H.E., 1987, Marching cubes: a high resolution 3D surface construction algorithm, *in* Association for Computing Machinery, SIGGRAPH: Computer Graphics, v. 21, p.163–169.

Mallet, J.L., 2004, Space-Time Mathematical Framework for Sedimentary Geology: Mathematical Geology, v. 36, p. 1-32.

Moore, G.E., 1965, Cramming More Components onto Integrated Circuits: Electronics, v. 38, p. 114-117.

Saad, Y., and Schultz, M.H., 1986, GMRES: a generalized minimal residual algorithm for solving nonsymmetric linear systems: Society for Industrial and Applied Mathematics, Journal on Scientific Computing, v. 7, p. 856–869.

Treece, G.M., Prager, R.W., and Gee, A.H., 1999, Regularized marching tetrahedral: improved iso-surface extraction: Computers and Graphics, v. 23, p. 583–598.

Turk, G., and O'Brien, J., 1999, Shape transformation using variational implicit functions, *in* ACM (Association for Computing Machinery) SIGGRAPH'99: Computer Graphics Proceedings, ACM Press, New York, p. 335–342.

Figures

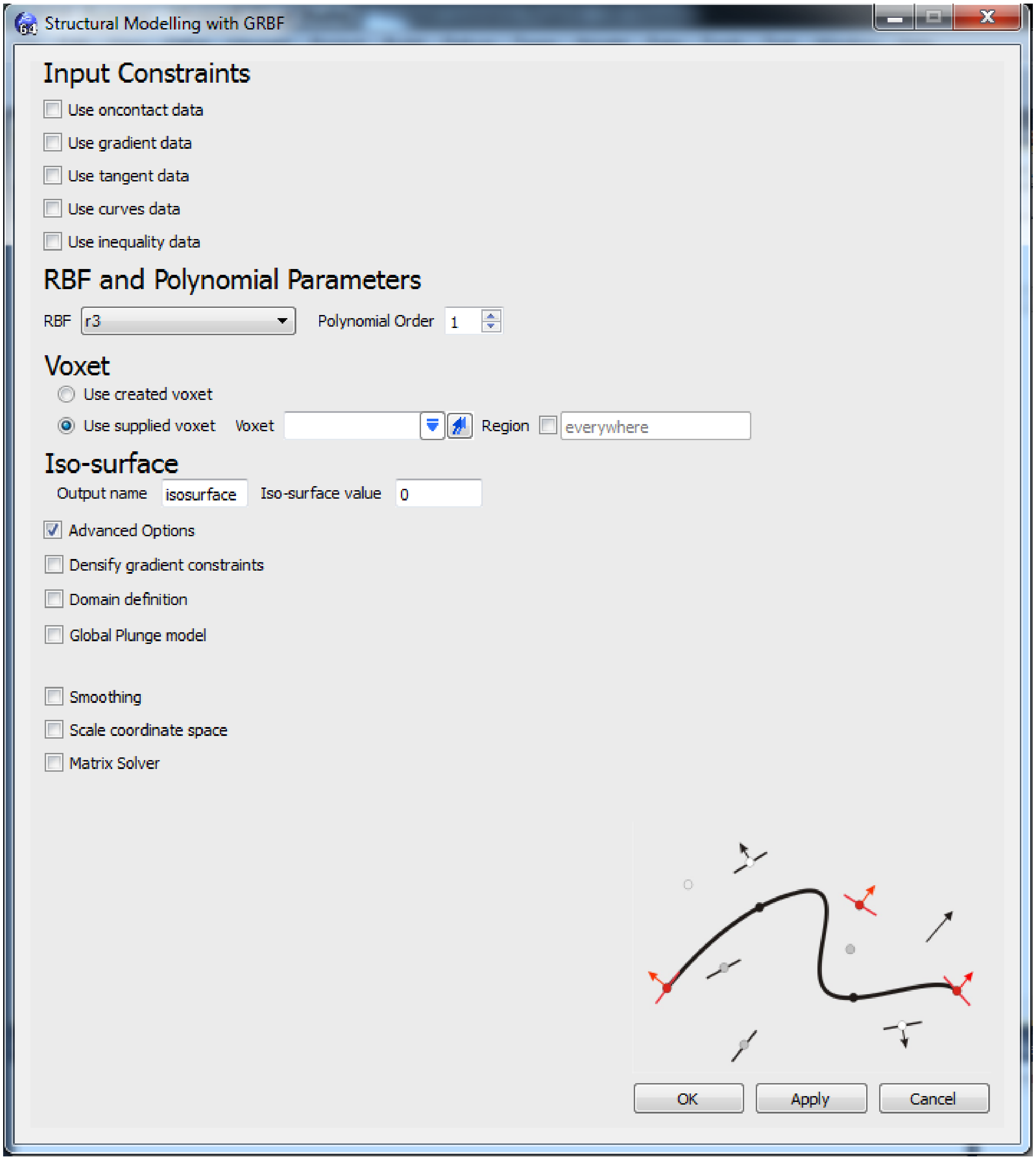

Figure 1. User interface for the generalized radial basis function GRBF algorithm plugin in Gocad/SKUA.

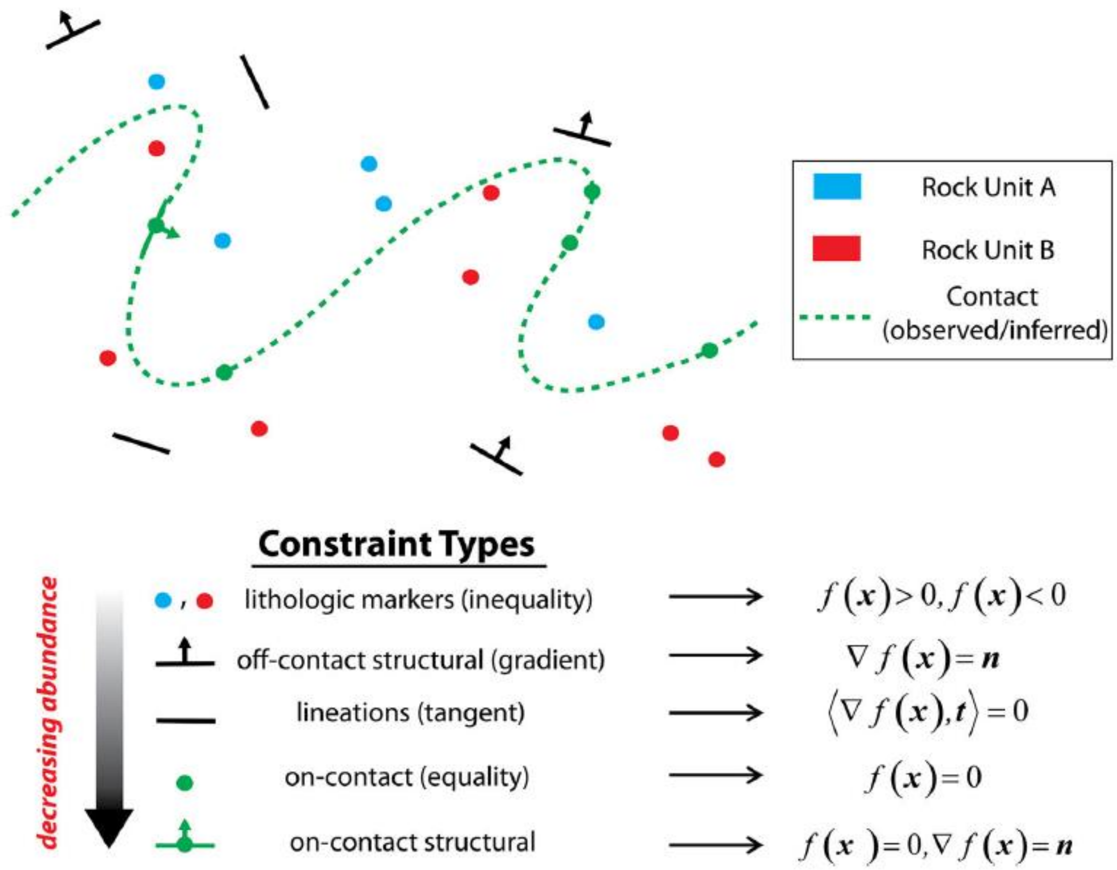

Figure 2. Structural constraint types used for implicit modelling in sparse environments. (Taken from Hillier et al., 2014)

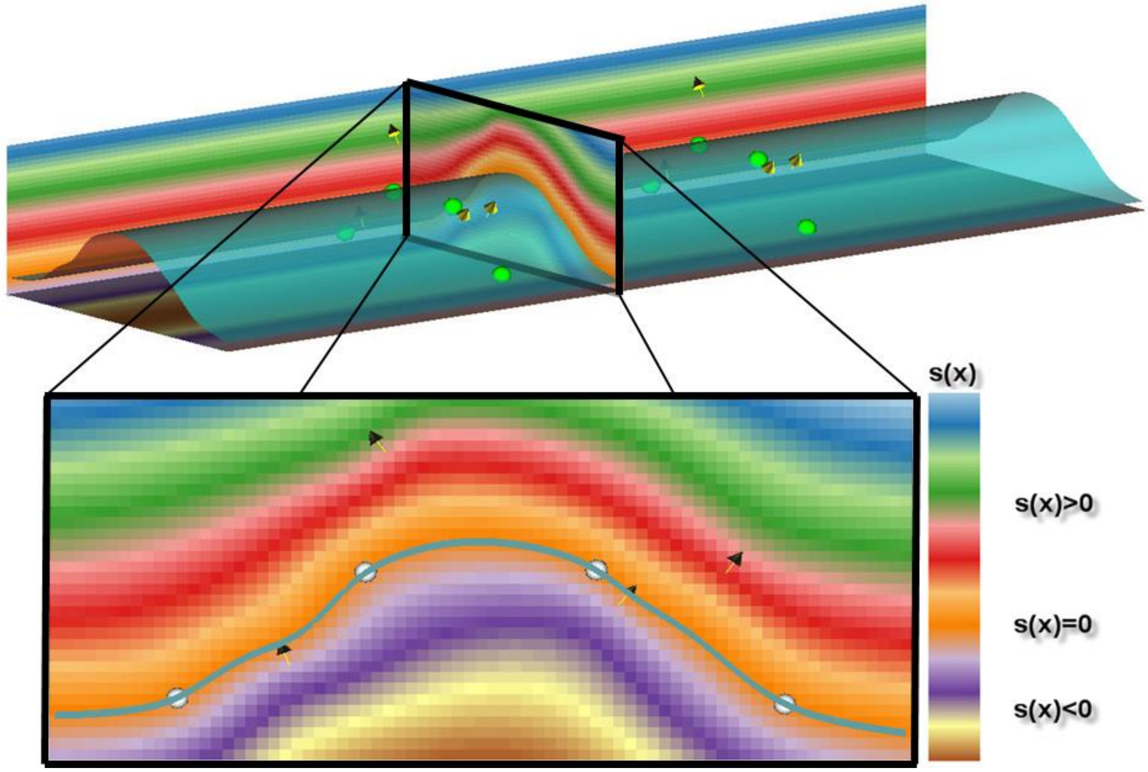

Figure 3. Scalar field for a synthetic anticlinal structure. (Top) 3D perspective with corresponding modelled surface extracted from 3D grid. (Bottom) Cross section view with scalar field colour map.

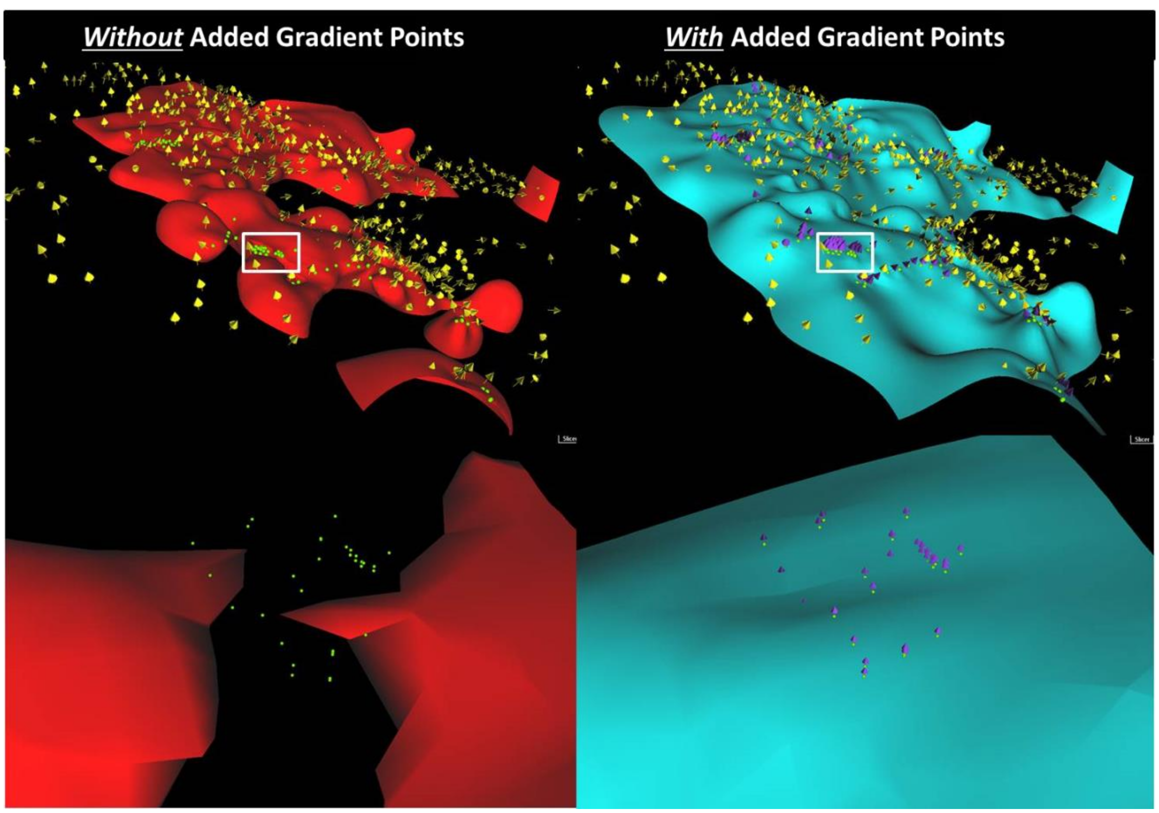

Figure 4. The effect of using the "densify gradient constraints" option on modelling results of the LMC horizon in the Purcell Basin. (Left) Not using the option and (Right) with using the option.

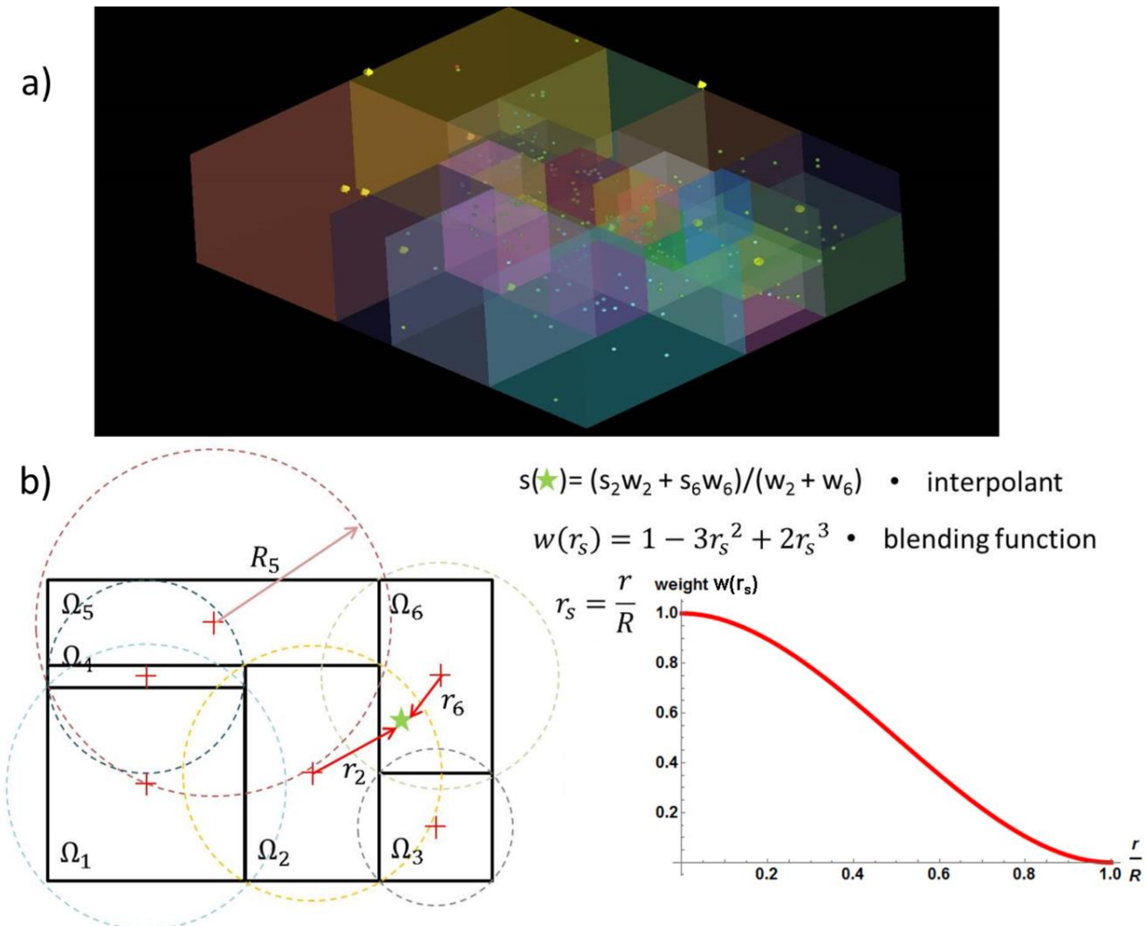

Figure 5. Domain decomposition method applied to GRBF (generalized radial basis function) interpolants. a) Visualization of 3D sub-domains generated from kd-tree algorithm. b) Partition of unity method.

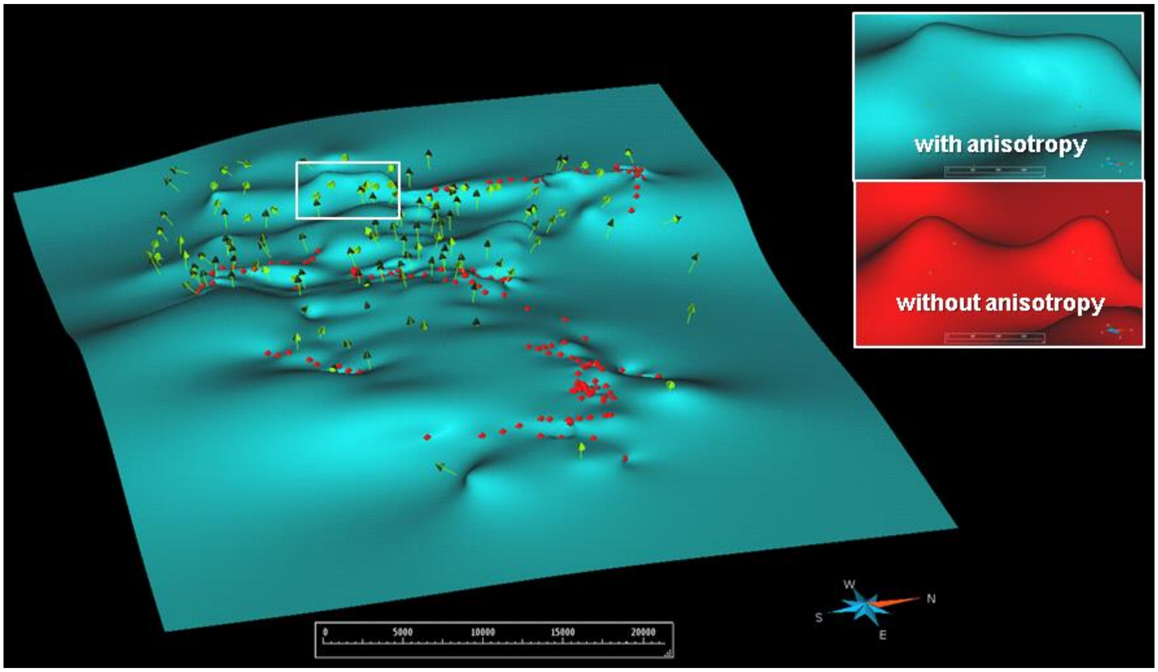

Figure 6. The effect of including global anisotropy on modelled results of LMC (Lower Aldridge-Middle Aldridge contact) in Purcell Basin.

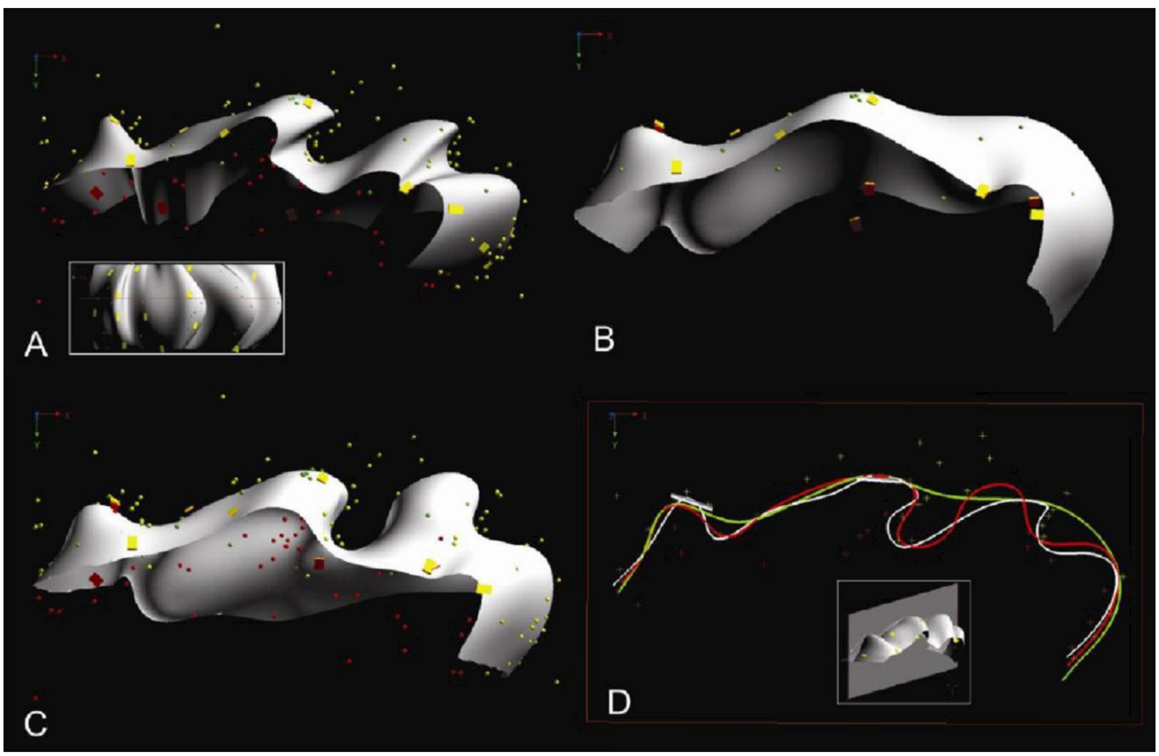

Figure 7. (A) Synthetic complex folded geological surface. (B) Modelled surface using sparsely distributed on-contact and gradient constraints. (C) GRBF modelled surface when inequality constraints, on-contact, and gradient constraints are included into the solution. (D) Cross-section comparison of the modelled (green (B) and red (C)) results with synthetic structure (white). (Taken from Hillier et al., 2014)

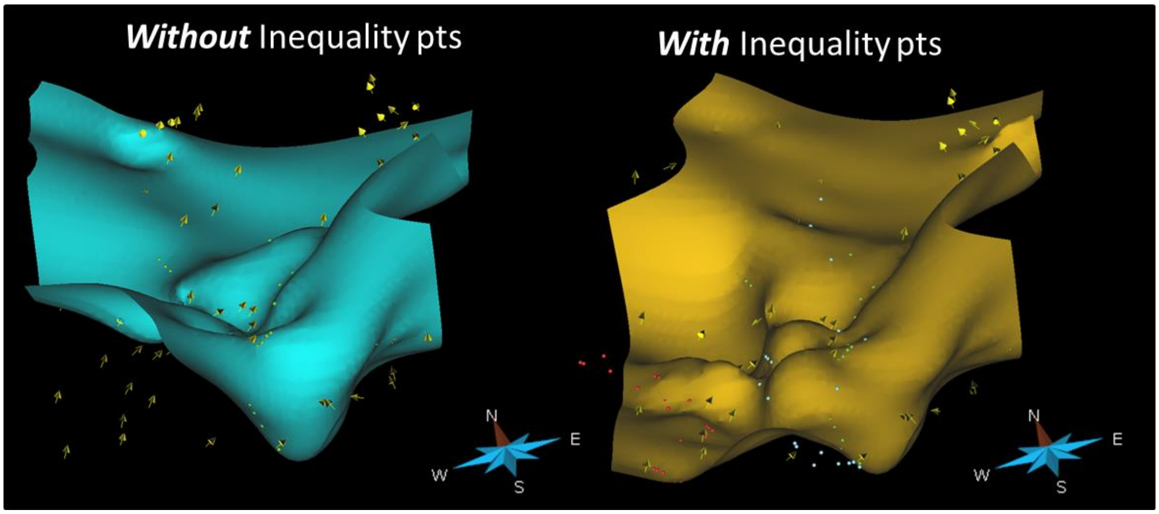

Figure 8. The effect of including inequality constraints into the generalized radial basis function (GRBF) algorithm on modelled geological surfaces.

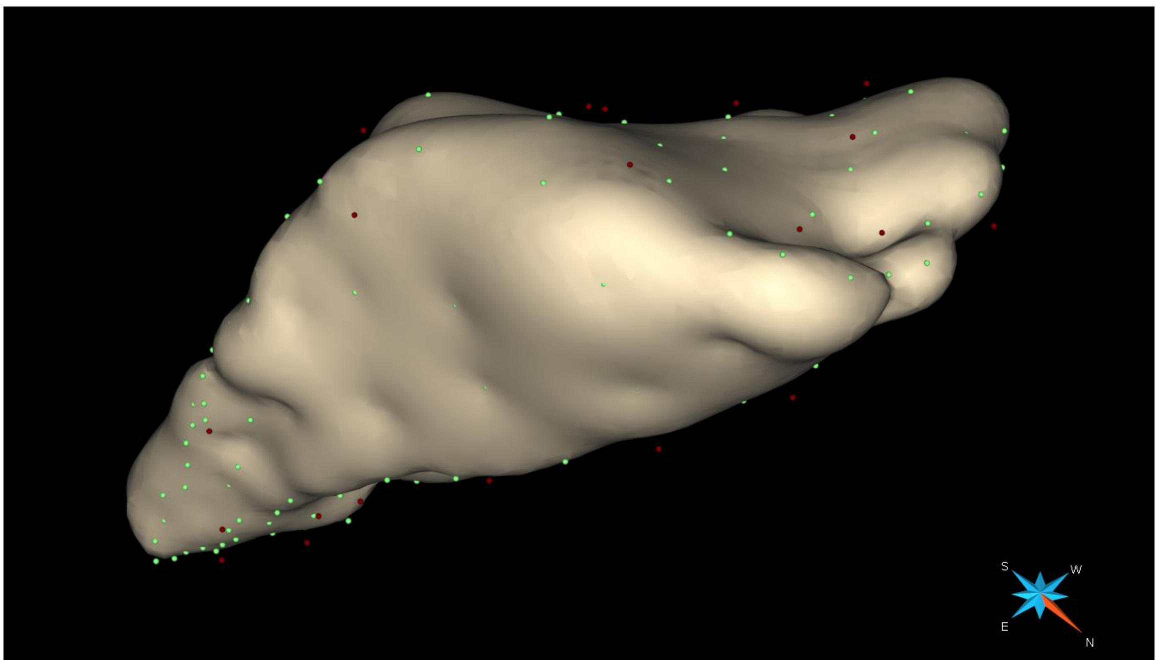

Figure 9. Modelled intrusion from point data sampling inside (blue – not visible), outside (red), and boundary (green) locations.

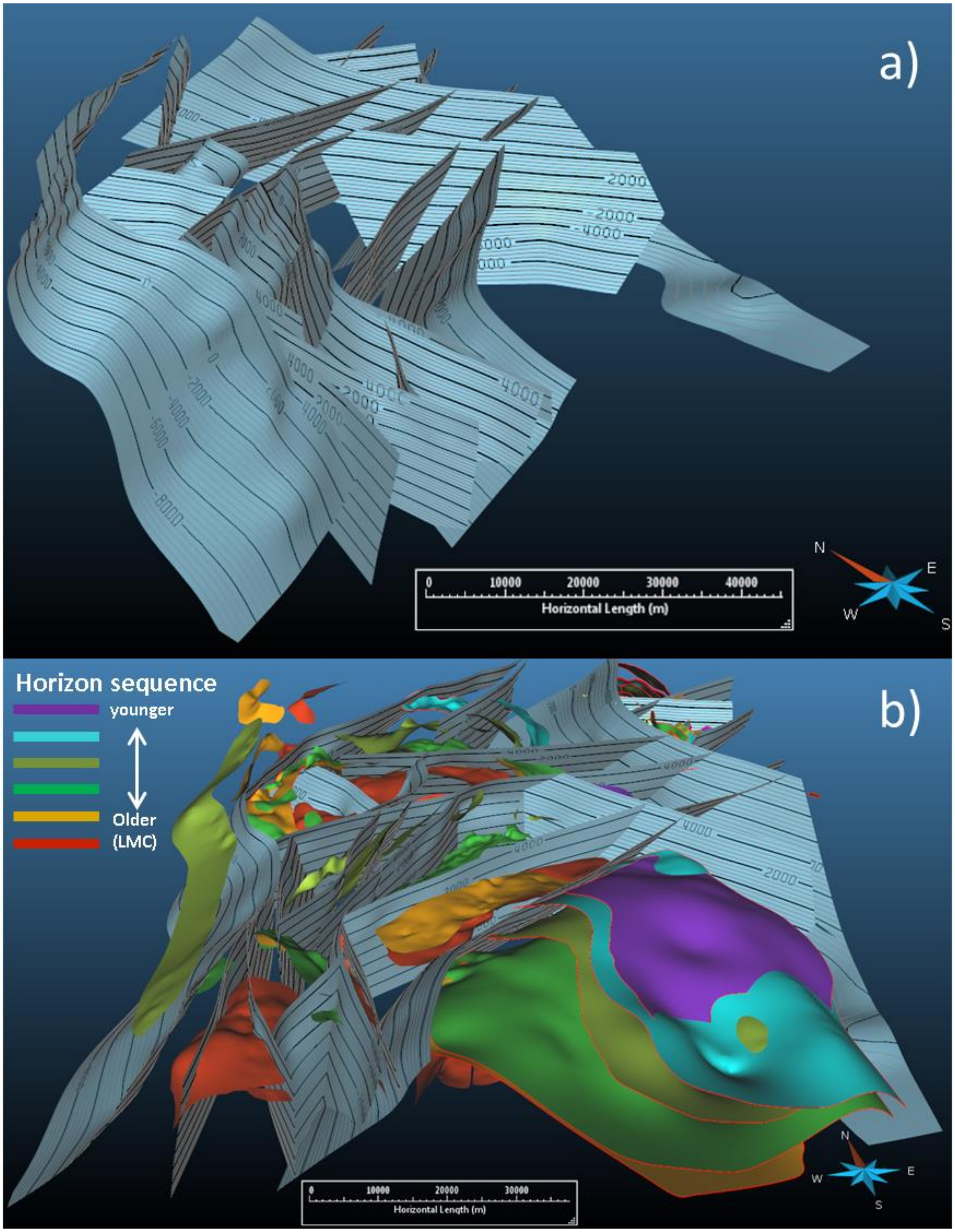

Figure 10. Generalized radial basis function (GRBF) modelling of the a) fault architecture and b) key stratigraphic horizons in the Purcell Basin. Elevation contours in metres, marked as black curves, are indicated on blue fault surfaces in (a). Lower Aldridge-Middle Aldridge contact (LMC) indicated in stratigraphic horizon sequence legend.

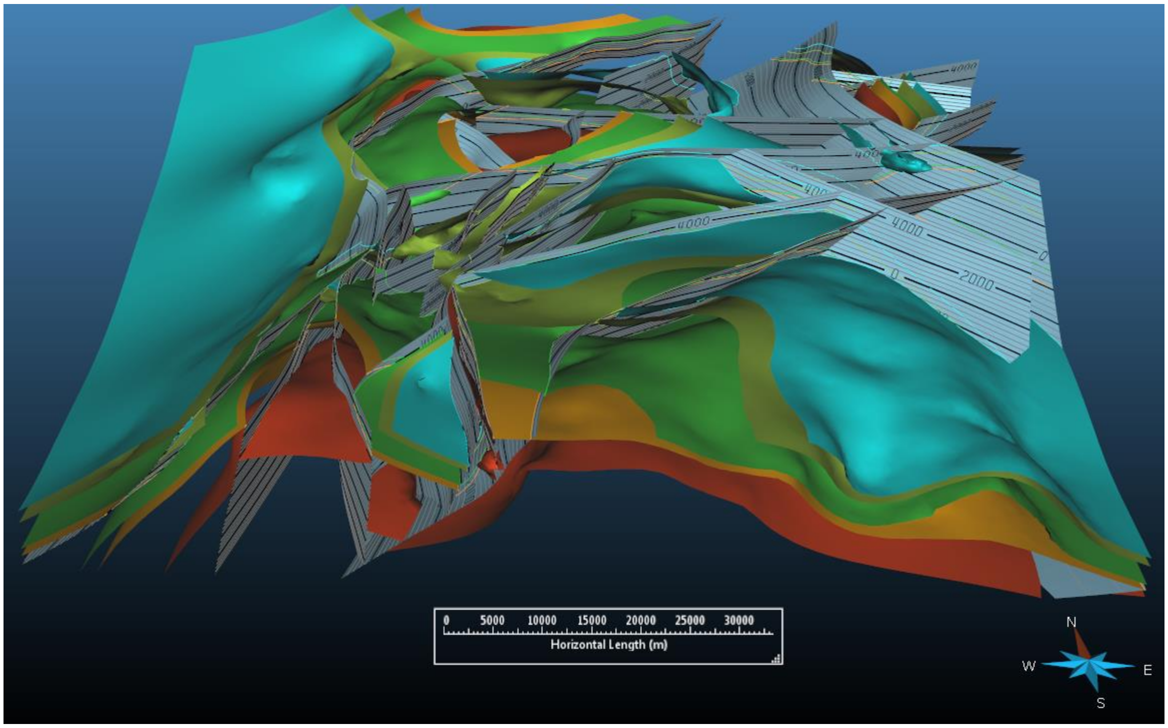

Figure 11. Final 3D structural model of key stratigraphic horizons in the Purcell Basin.